Central Sands的水文地质环境

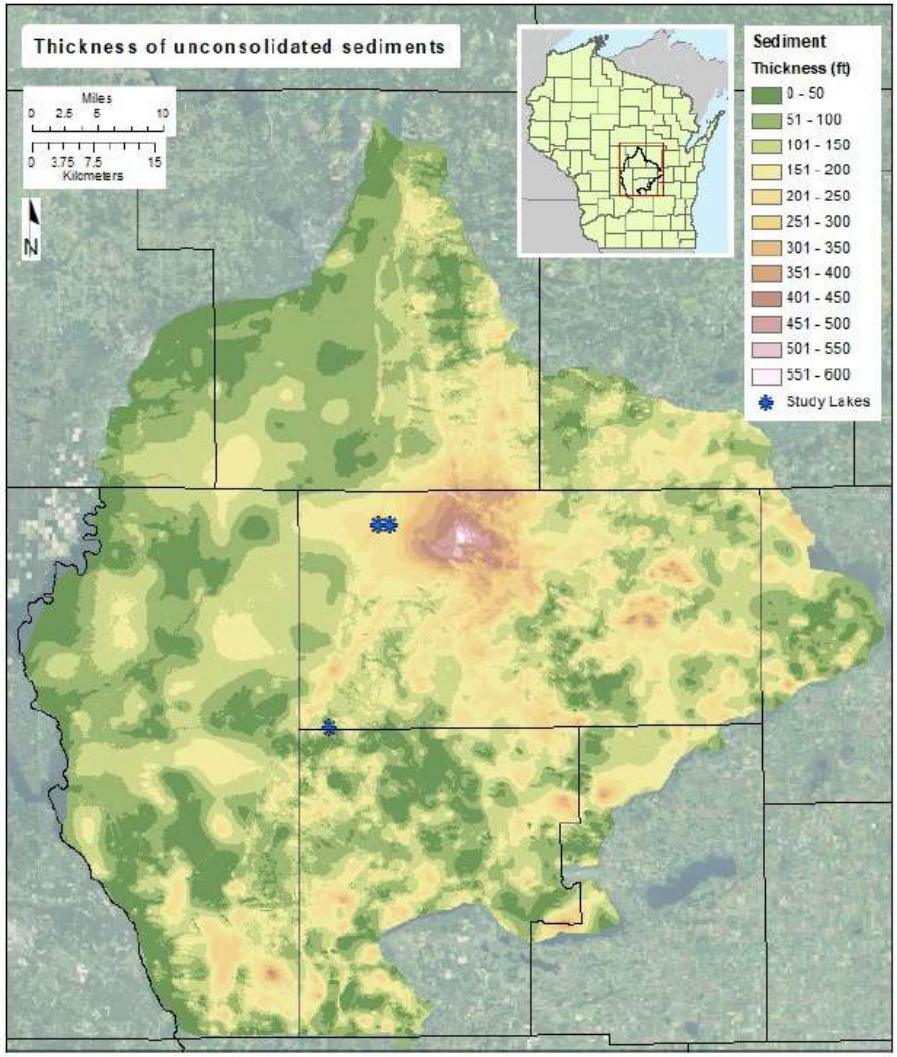

含水层厚度约15 m

图2 模型区域内沉积物厚度
厚度是由从LiDAR的DEM减去插值的基岩表面高度得到。泥沙类型间厚度差异不显著。

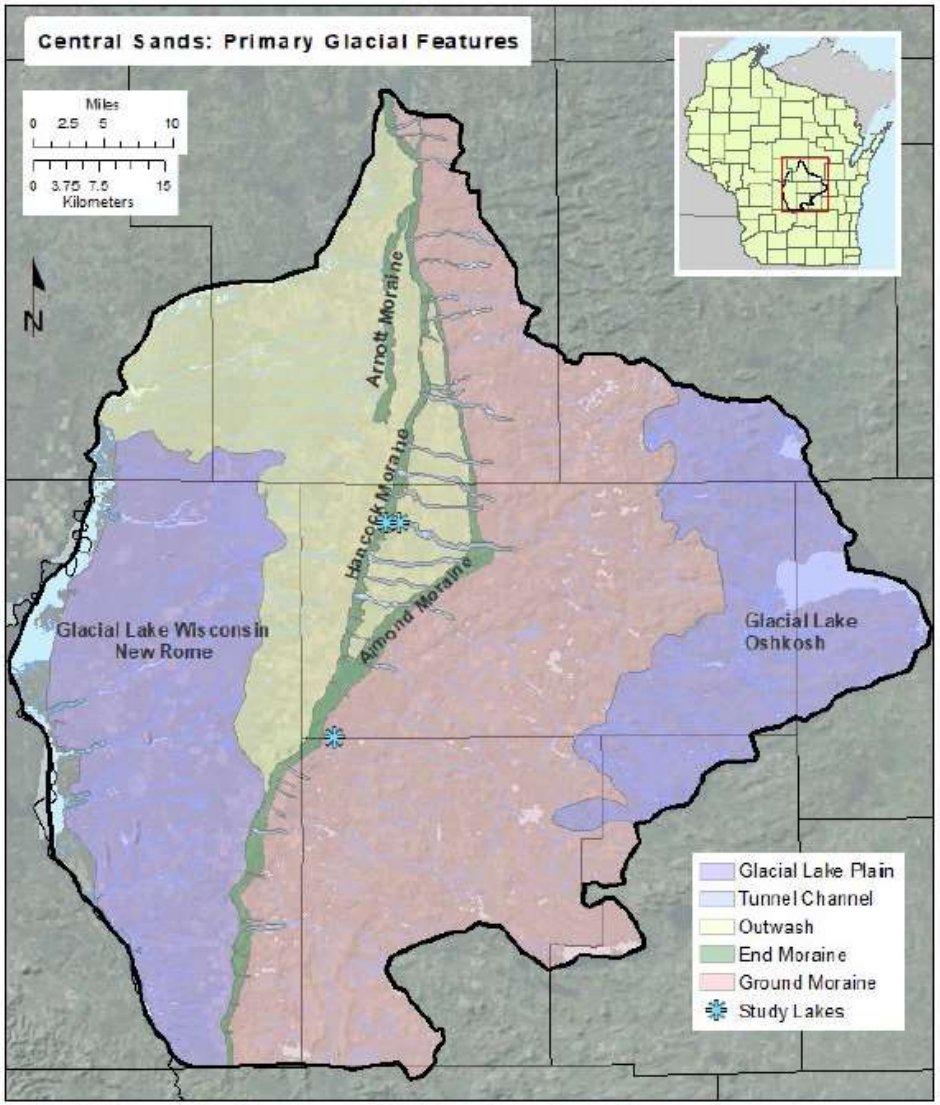

Figure 3. Primary glacial features of the Central Sands model domain.

图3 研究区域的冰川地质特性

基岩地质

主要的基岩含水层是Cambrian sandstone，厚度分布极不均匀（0~30m）

sandstone含水层下面是Crystalline基岩，可认为是不透水层。

carbonate基岩，没有出现在地下水位以下。

数据收集与分析

using geophysics, geologic logging, aquifer tests, groundwater-level monitoring, a canoe-based survey of lake chemistry, temporary lakebed piezometers, and seepage meters

使用收集的数据，创建模型分层，定义含水层特定的合理取值范围，为地下水模型提供近场参考水头数值。

井

30064个测井，描述地下水分布。

图9, 9982个浅水层水井，2368个基岩井，获得地下水位。

除了创建地质分层和参考水头值，还可计算水力传导度（见Aquifer Properties讨论）。

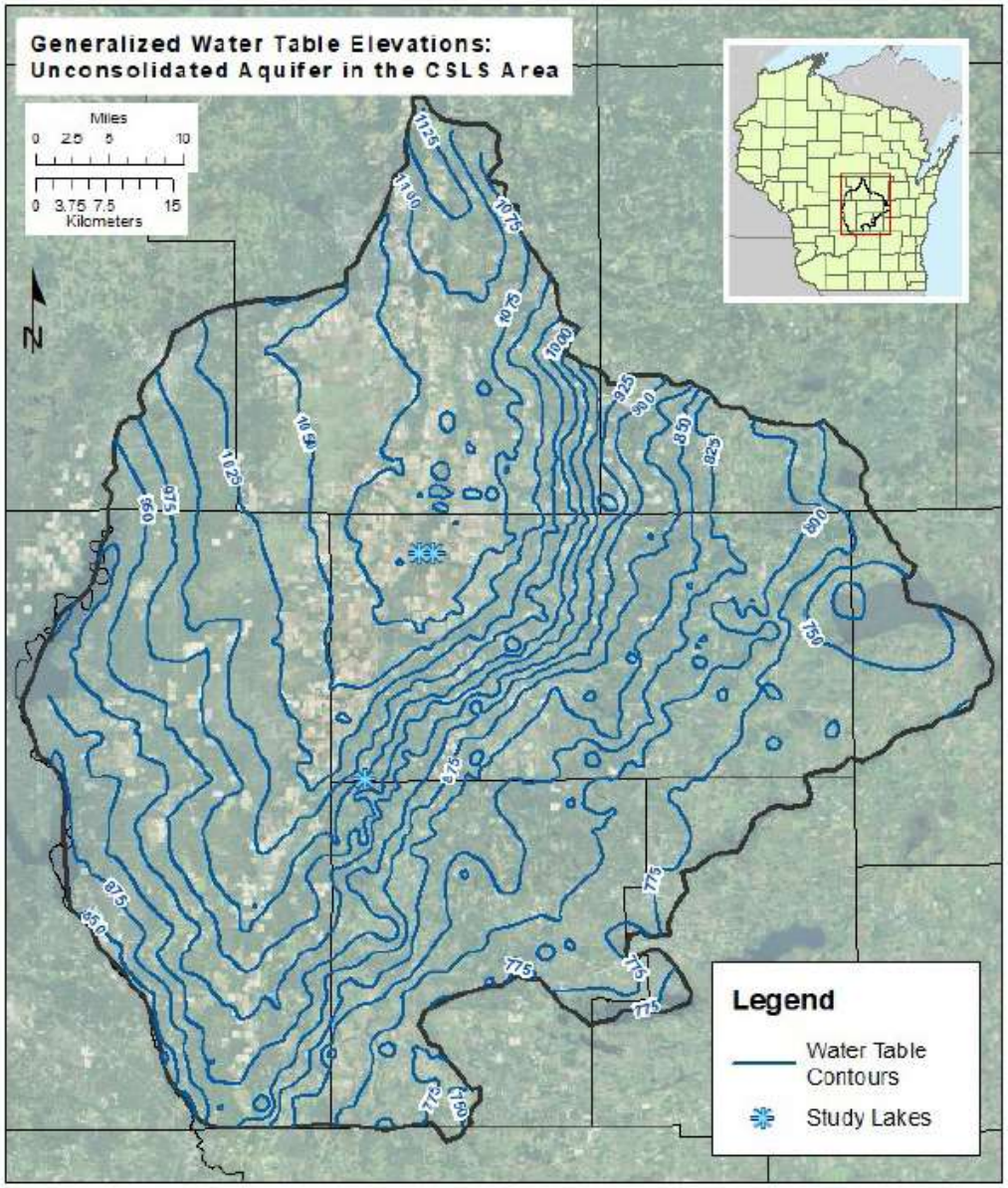

图9, 9982个浅水层水井，2368个基岩井，获得地下水位。

地球物理探测

•使用地震波评估到基岩的深度（在钻孔和深井稀少的区域），地震剖面主要集中在研究湖泊周围区域。

•在重点区域，直接使用渗透仪器，测量水平和垂向水力传导度的变化。

•使用gamma logging确认钻孔的细粒度沙区域。

•使用穿地雷达(GPR)补充Long Lake的地质钻孔数据，确认浅层细粒度沙子的范围和组成。

地球物理探测

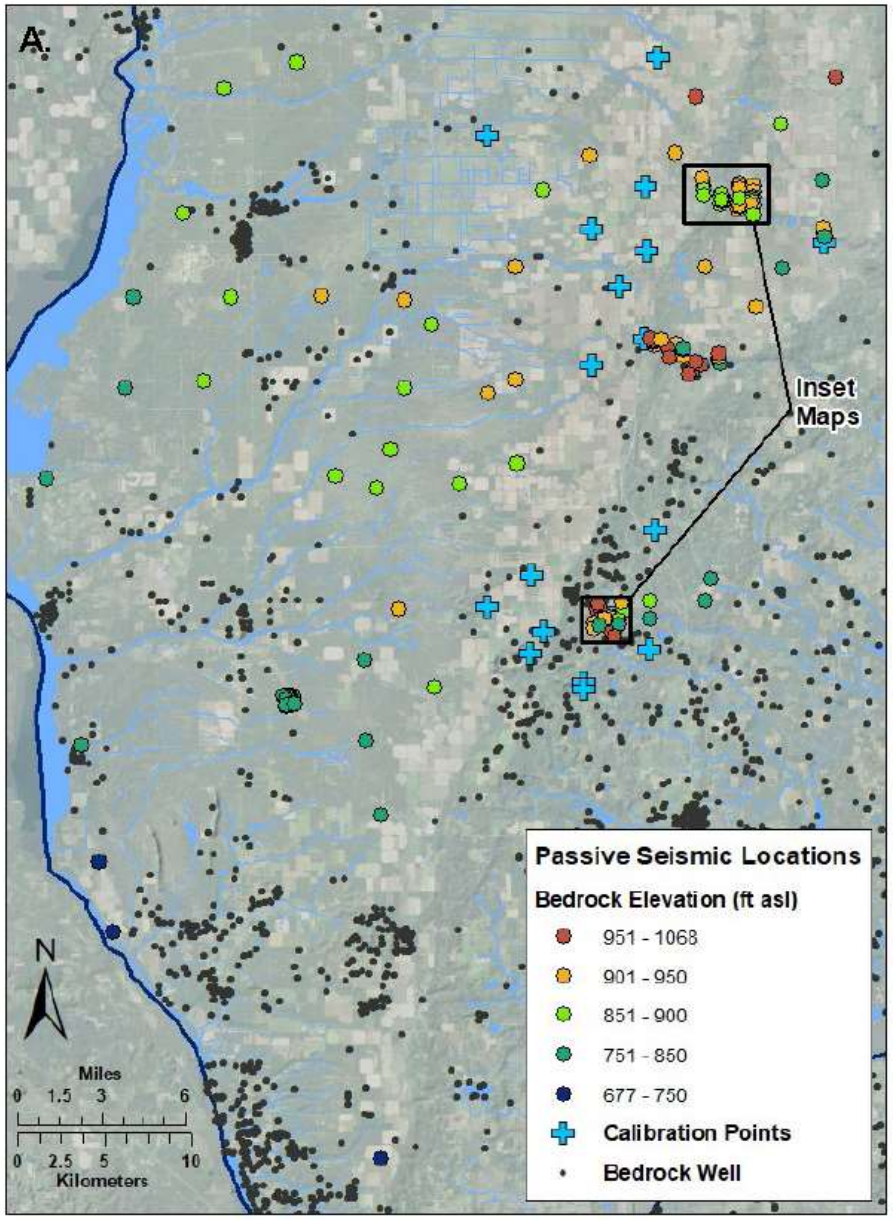

图11(a) 地震剖面测量位置和率定点，显示了测井相对基岩的深度信息，地震数据主要集中在基岩深度很浅的区域

地球物理探测

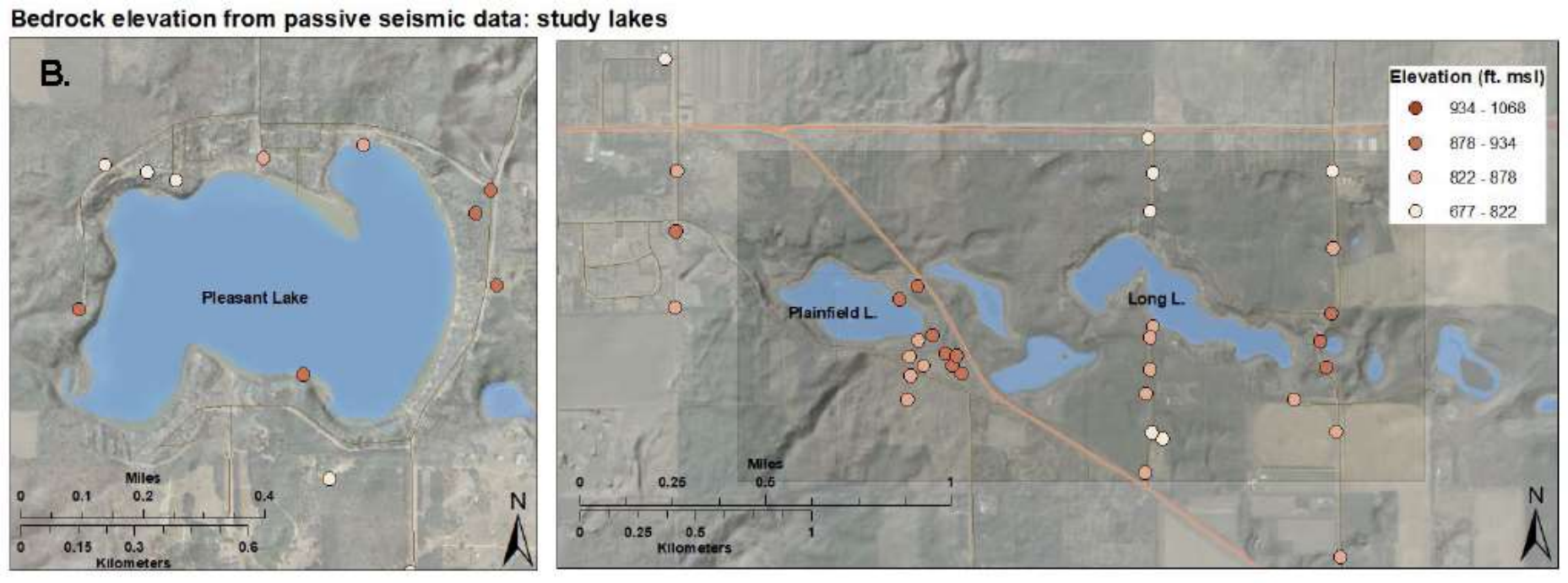

图11(b)研究湖泊周围的地震勘探

Down-hole地球物理

Gamma Log，提供岩石地层信息。 图17

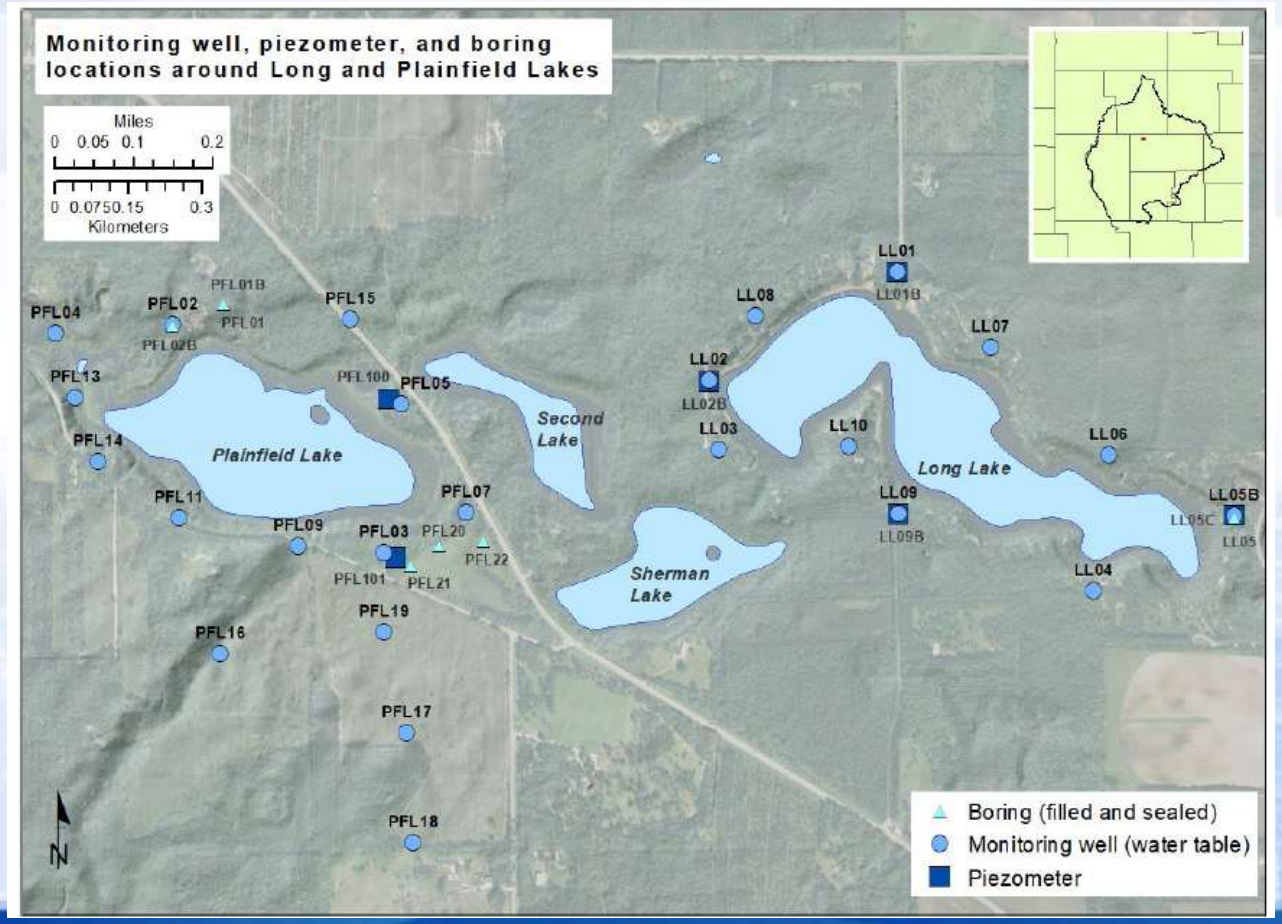

穿地雷达(GPR)

在Long Lake西南边，图15和图16，地表以下近20m深度。

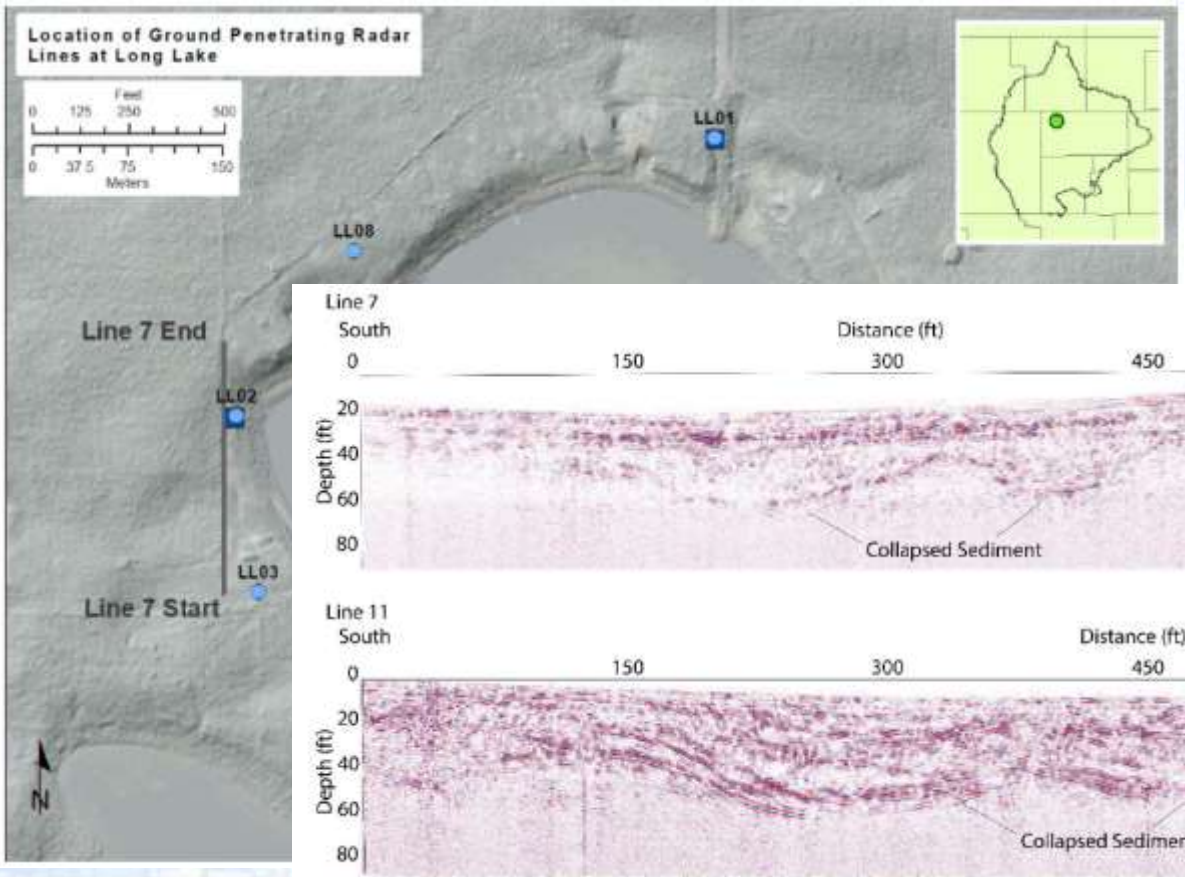

Figure 16. GPR records along Lines 7 and 11. The collapsed sediment is apparent in both lines. The water table in Line 7 is also indicated.

Plasant湖周围的钻孔（观测井）

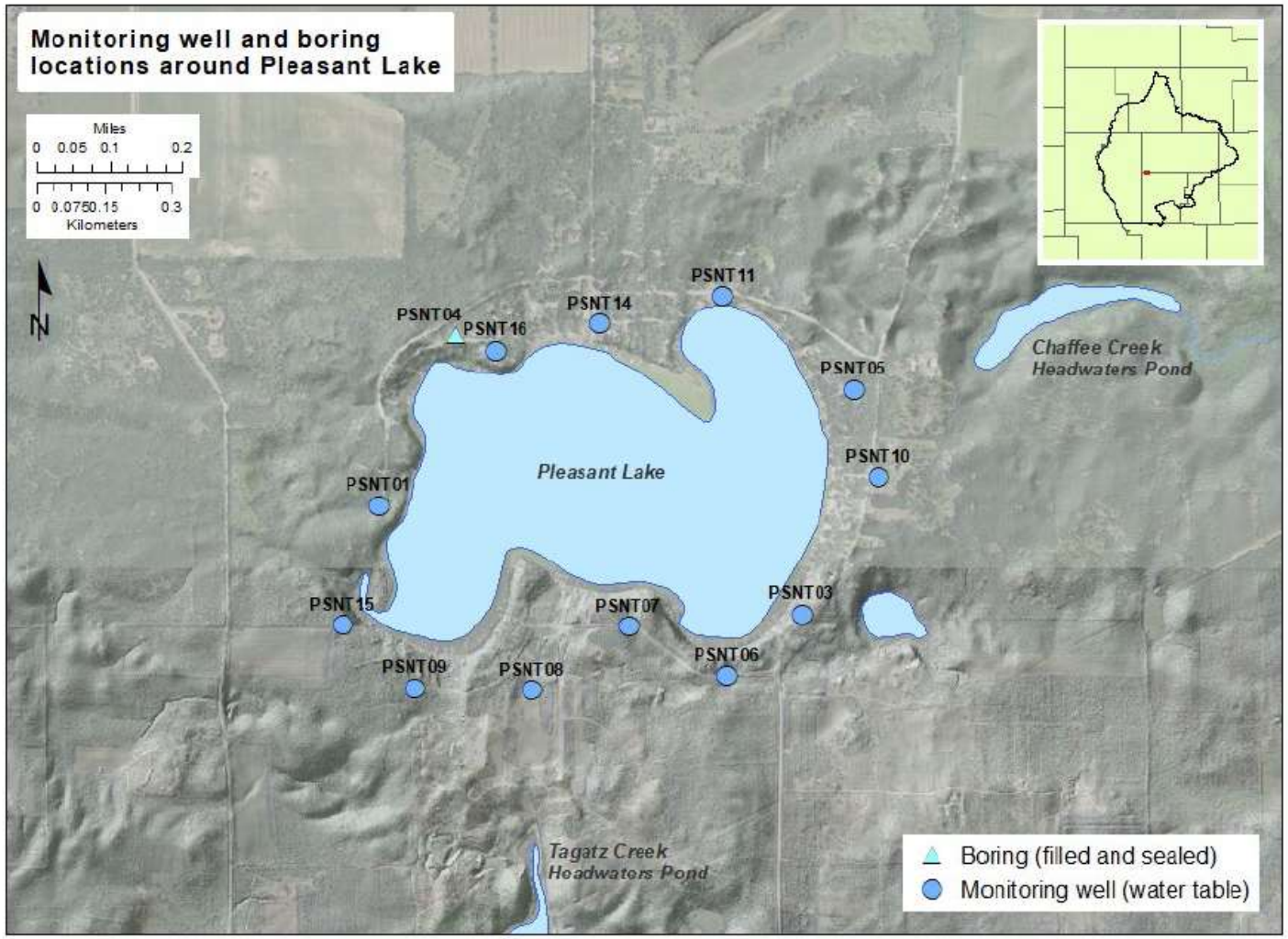

Plasant湖周围的钻孔（观测井）

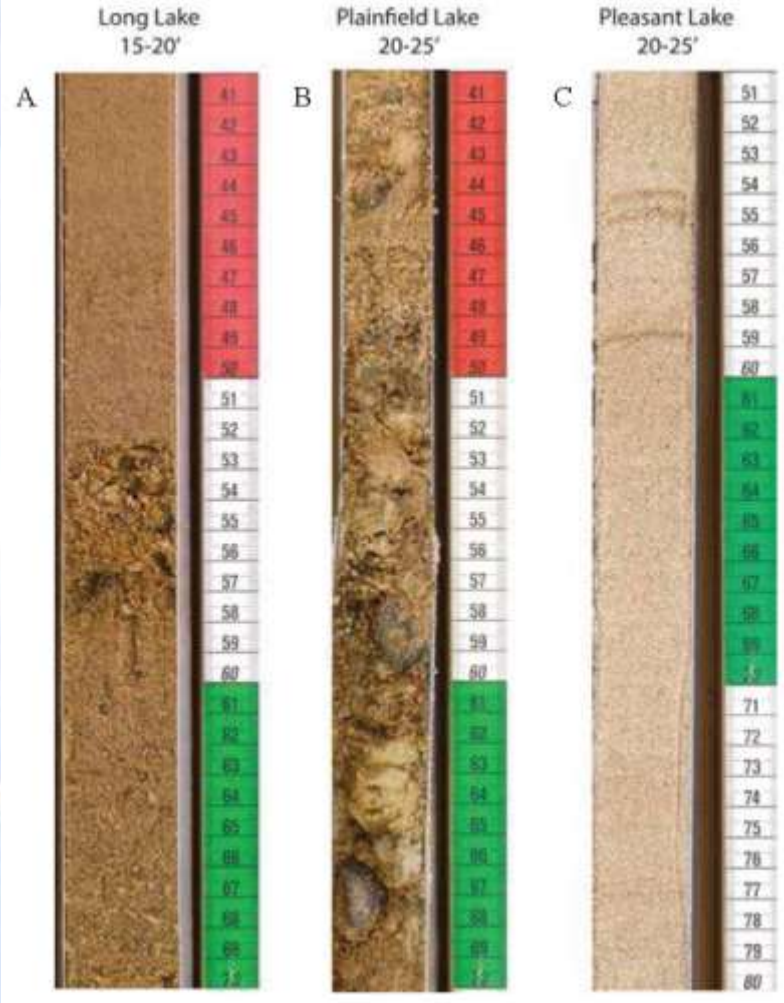

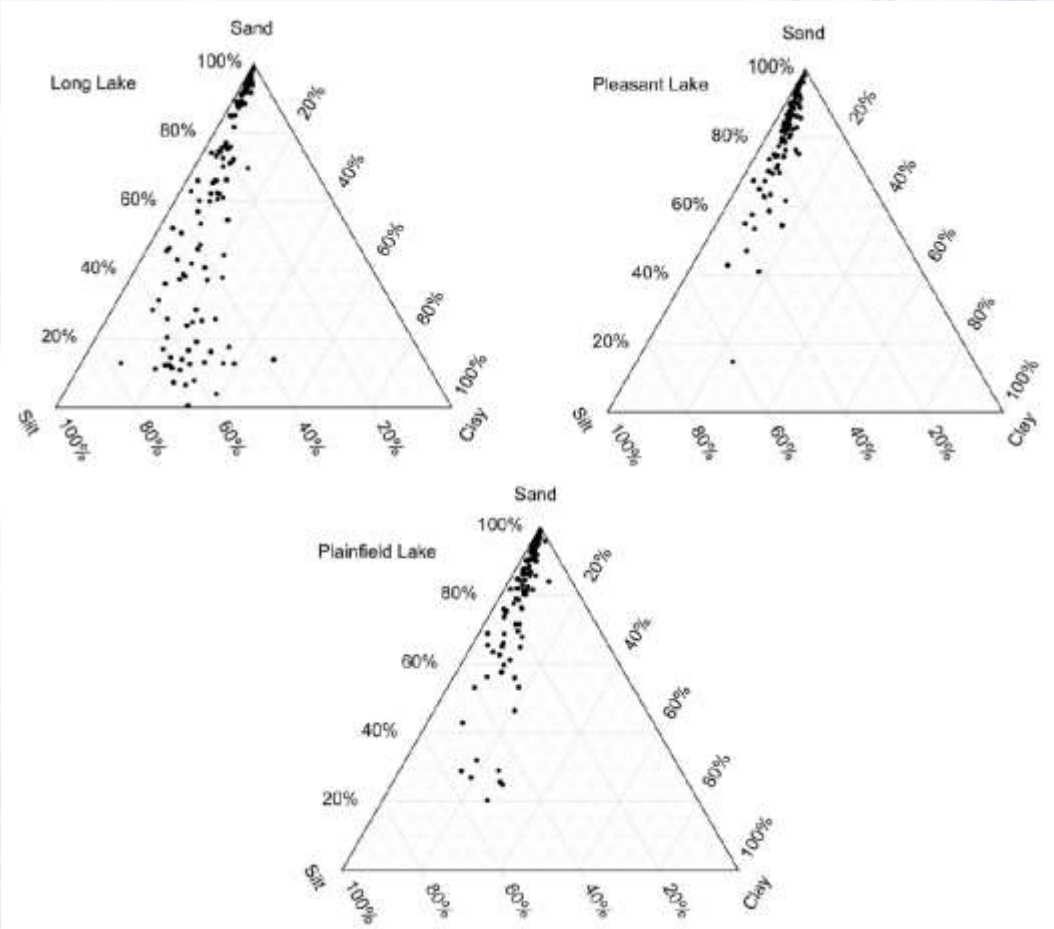

含水层试验（水力传导度）

平均的水力传导度是106ft/d （slug test）
平均的水力传导度是234ft/d (pumping test)
非承压sand and gravel含水层有平均值0.17
垂向水力传导度其$2.6x10^{-5}$ft/d，到0.56ft/d(aquifer loading)。

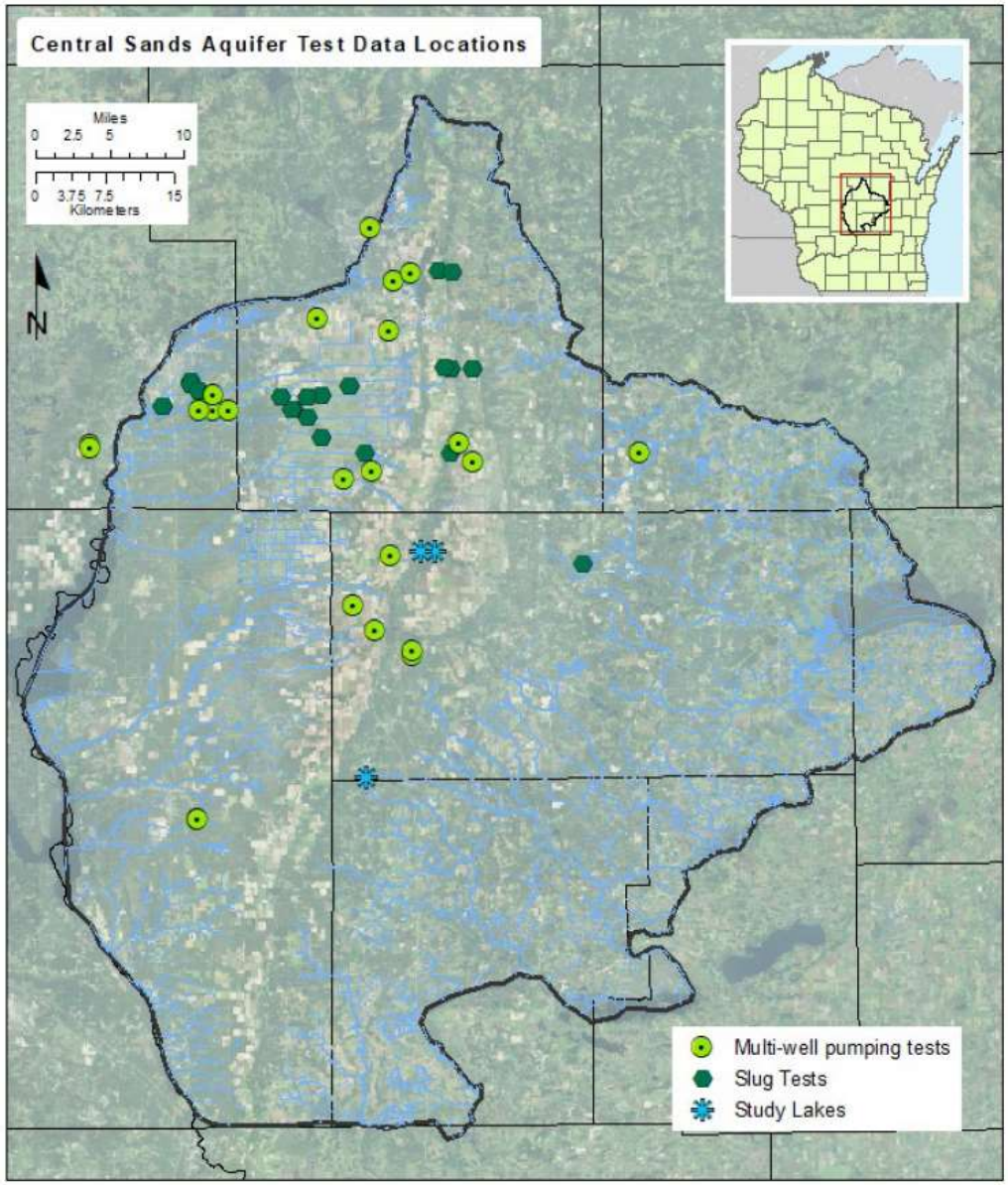

含水层试验（水力传导度）

Table 1. Summary of previously published aquifer property values, CSLS model domain

	Horizontal Hydraulic Conductivity (ft/d)			
	Piezometer-slug tests	*Multi-well pumping tests*	*Anisotropy Kh:Kv*	*Specific Yield*
n	*46*	*24*	*5*	*20*
Min	0.7	66	1:1	0.026
Max	270	500	20:1	0.33
Mean	106	234	7:1	0.17

Table 2. Hydraulic conductivity by geographic region. Data source is WCR specific capacity tests. Hydraulic conductivity was calculated using TGUESS. Because the hydraulic conductivities have log-normal distribution, standard deviation of log K is reported.

		Mean K (ft/d)	*Range (ft/d)*	*Standard Deviation of log K*	*n*
Bedrock		15	*0.001-1925*	*1.00*	*16,726*
Unconsolidated	Outwash Plain	158	*0.008-19,049*	*0.42*	*4255*
	Intermoraine	172	*0.85-812*	*0.41*	*582*
	Glacial Lake Wisconsin / New Rome	120	*0.04-1965*	*0.49*	*3285*
	End Moraines	156	*0.5-2149*	*0.52*	*590*
	Tunnel Channels	156	*0.78-1325*	*0.49*	*323*
	Ground Moraine	112	*0.03-3961*	*0.47*	*9392*
	Glacial Lake Oshkosh	78	*0.66-1985*	*0.46*	*1067*

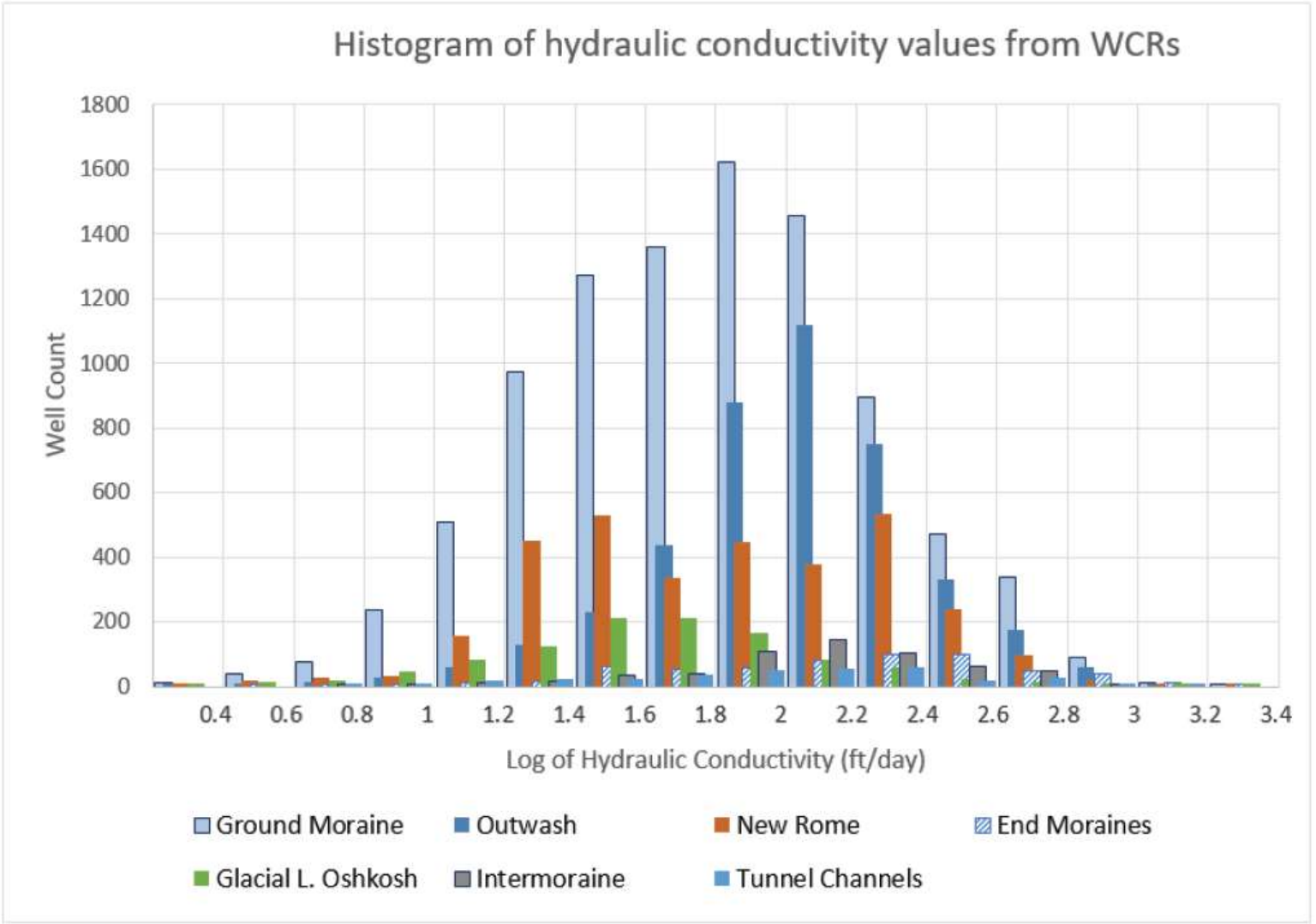

Figure 30. Summary of hydraulic conductivity distribution from specific capacity tests in unconsolidated sediments.

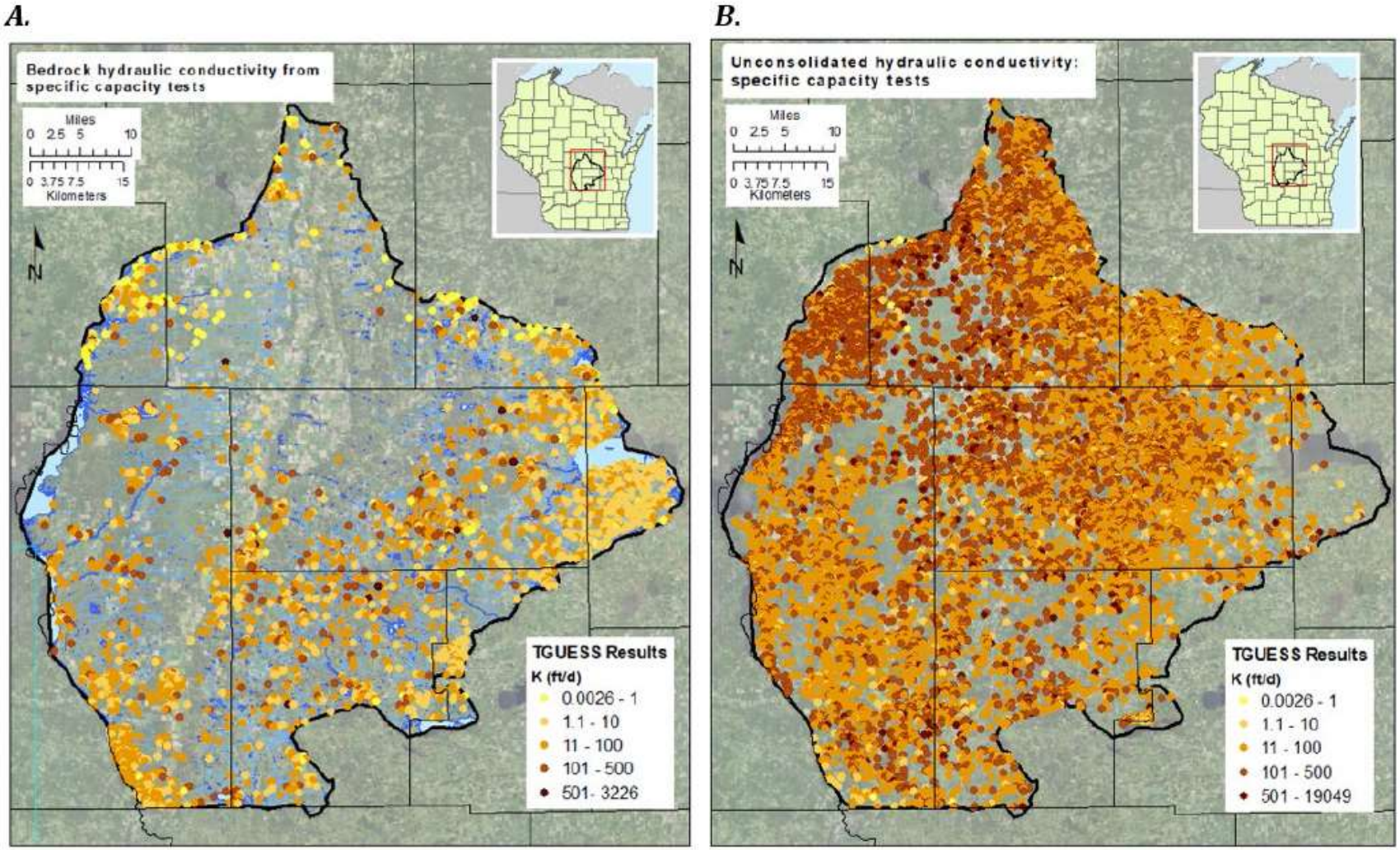

Figure 31. Hydraulic conductivity values from specific capacity tests (via TGUESS) (a) Bedrock points (b) Unconsolidated points. Bedrock conductivities are typically an order of magnitude lower than conductivity in the sand and gravel aquifer. The highest conductivities are in the outwash plain west of the Almond Moraine.

含水层特性测试—观测井

	Hydraulic Conductivity (ft/d)			
	Range	*Mean*	*Median*	*n*
Long L.	7.3-69	39	39	14
Plainfield L.	72.6-637	168	105	10
Pleasant L.	24-130	73	60	12

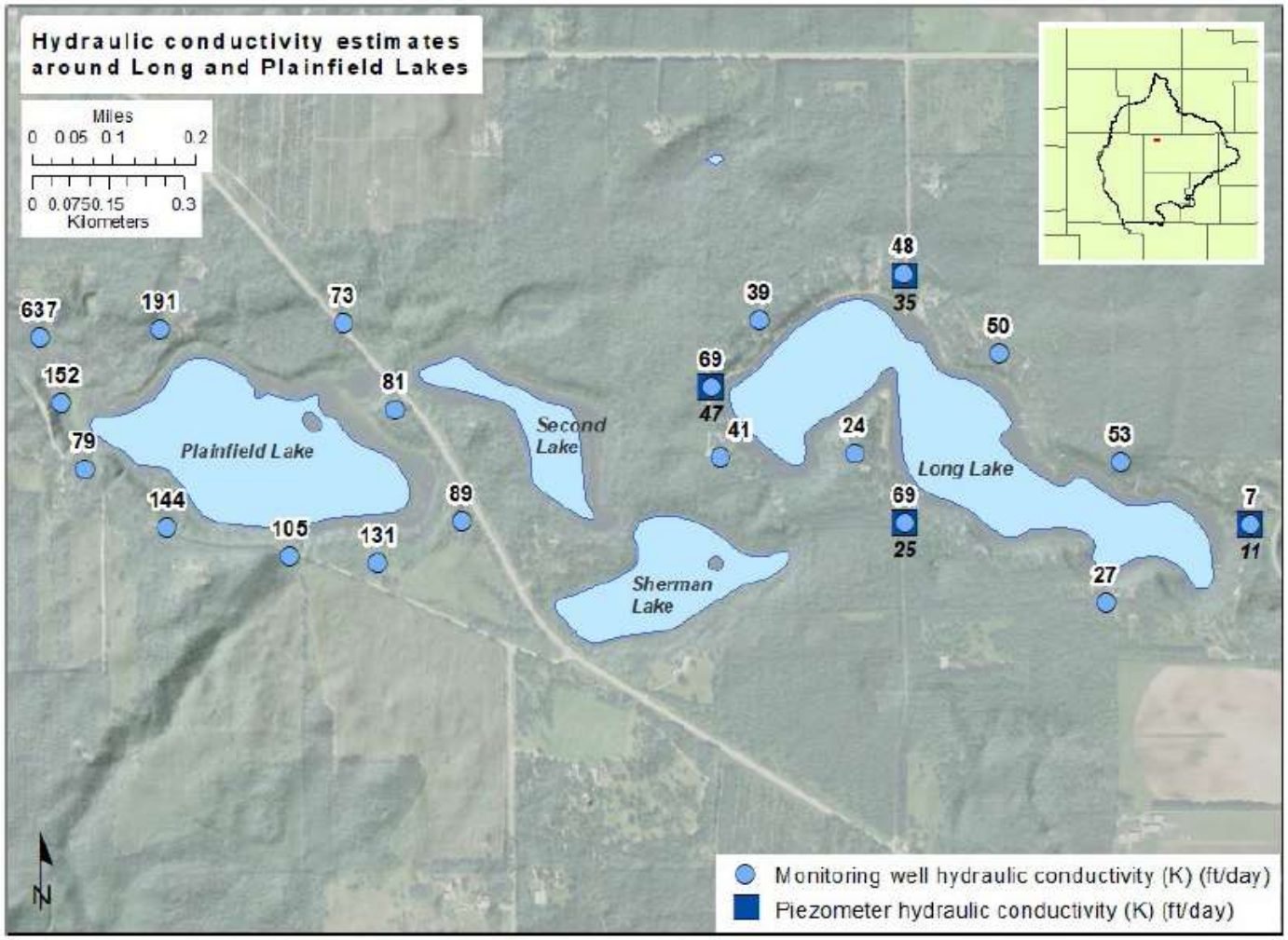

Figure 32. Hydraulic conductivity estimates for monitoring wells and piezometers around Long and Plainfield Lakes. Values for piezometers are in italics below the corresponding symbol. All values are in ft/d.

研究湖泊周围的水文：地下水位观测

方法：钻孔、观测井和piezometer安装

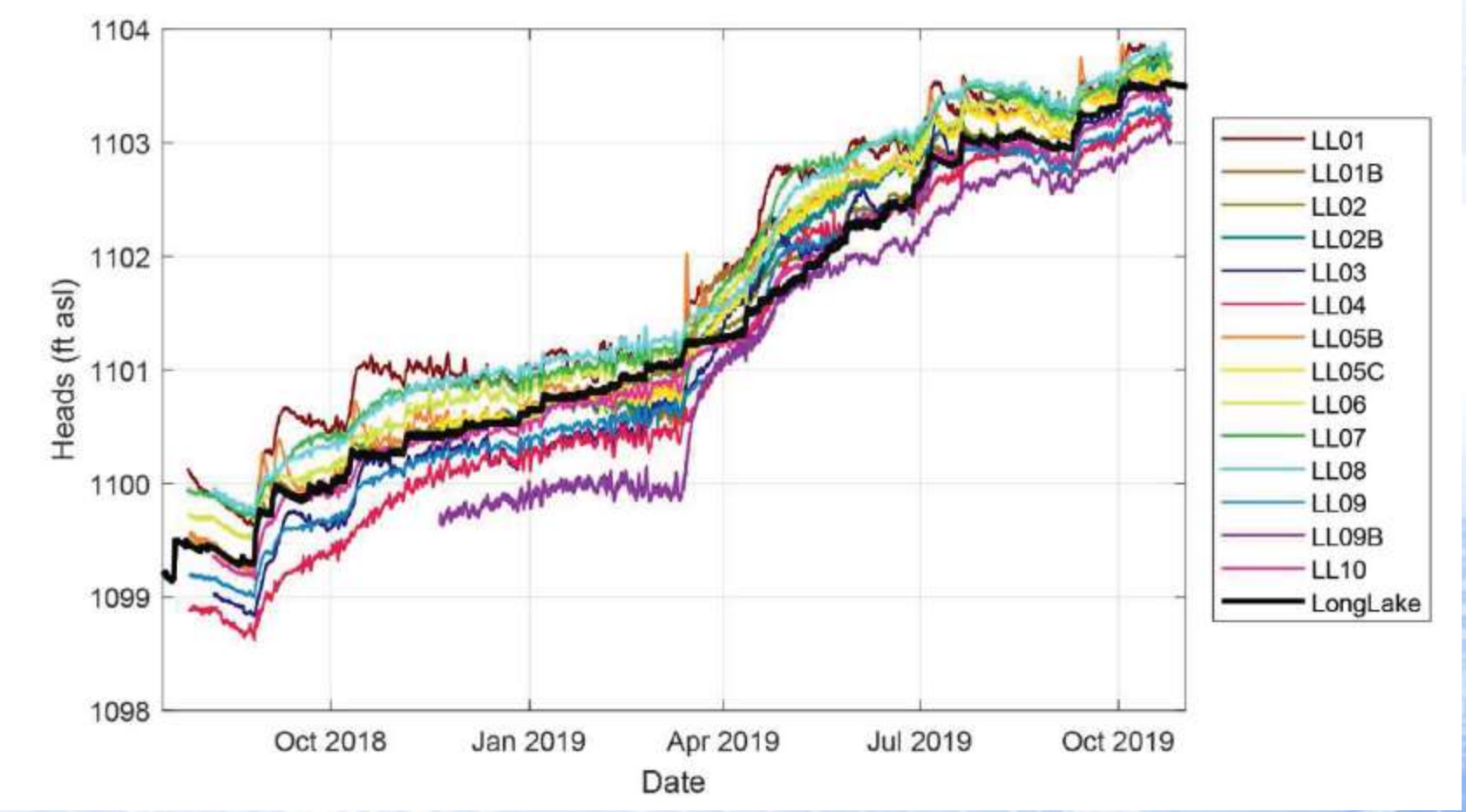

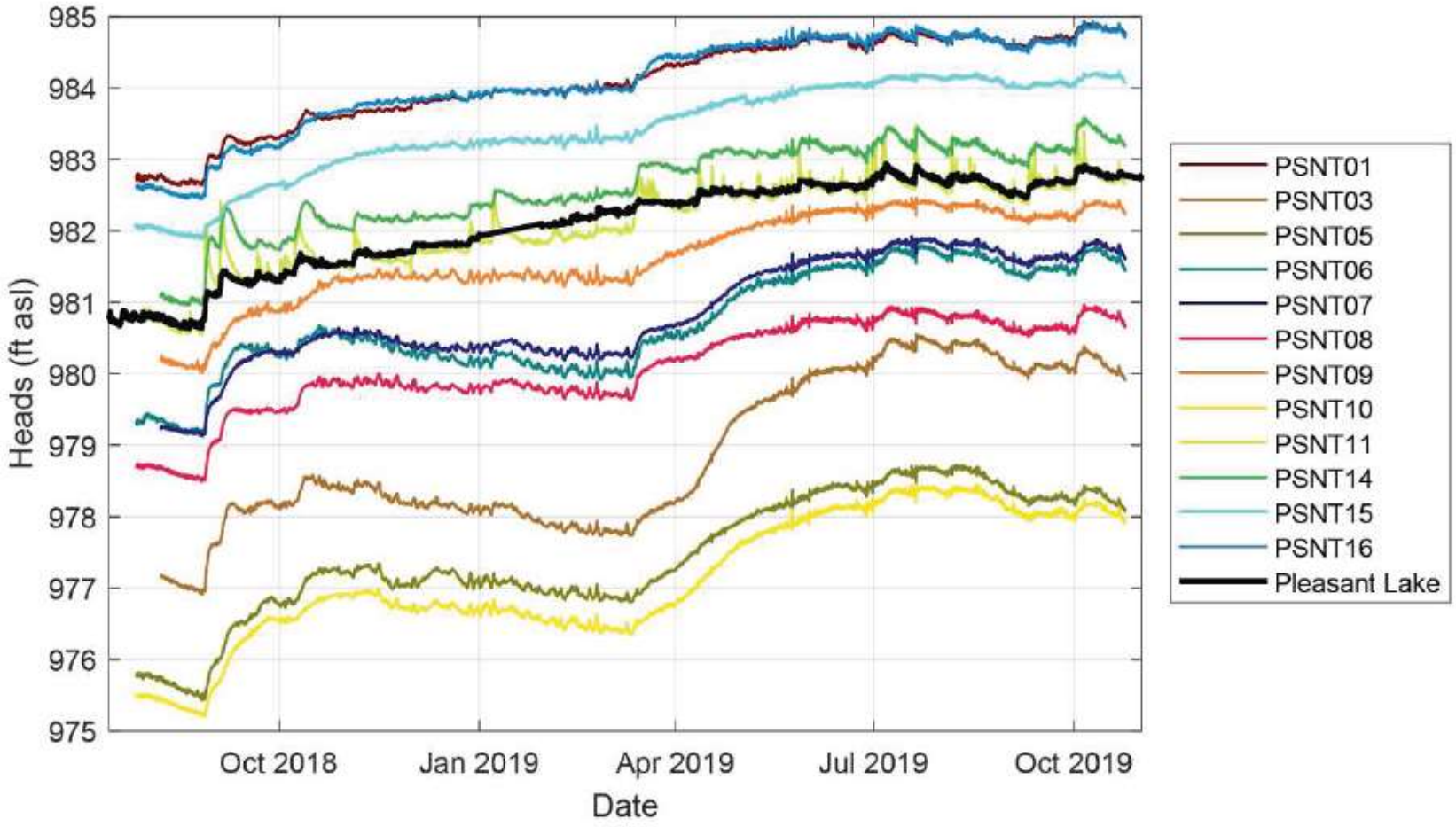

Figure 36. Groundwater levels in monitoring wells around Pleasant Lake from summer 2018 to fall 2019. Lake-level elevation is shown in black. Overall increase in water levels is approximately 2 ft over this 15-month period.

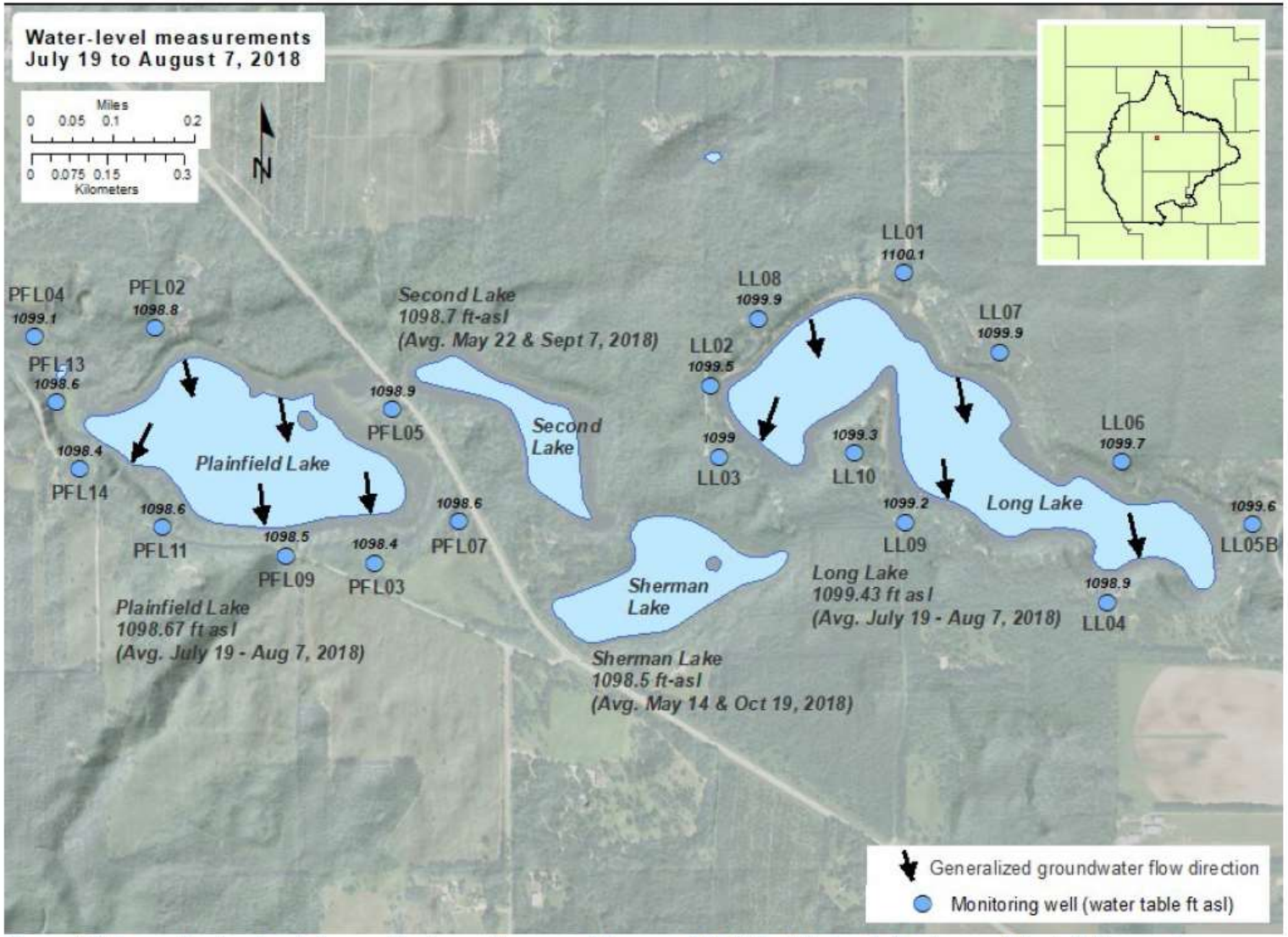

Figure 37. Groundwater levels in monitoring wells around Long and Plainfield Lakes following well installation and development in July and August 2018. Levels shown for Long and Plainfield Lakes are averages of continuous 15-minute USGS gaging station data published on their National Water Information System (NWIS) web interface. Levels reported for Second and Sherman Lakes are averages of two periodic WDNR measurements published on their Surface Water Data Viewer and represent more generalized water levels.

垂向水力梯度

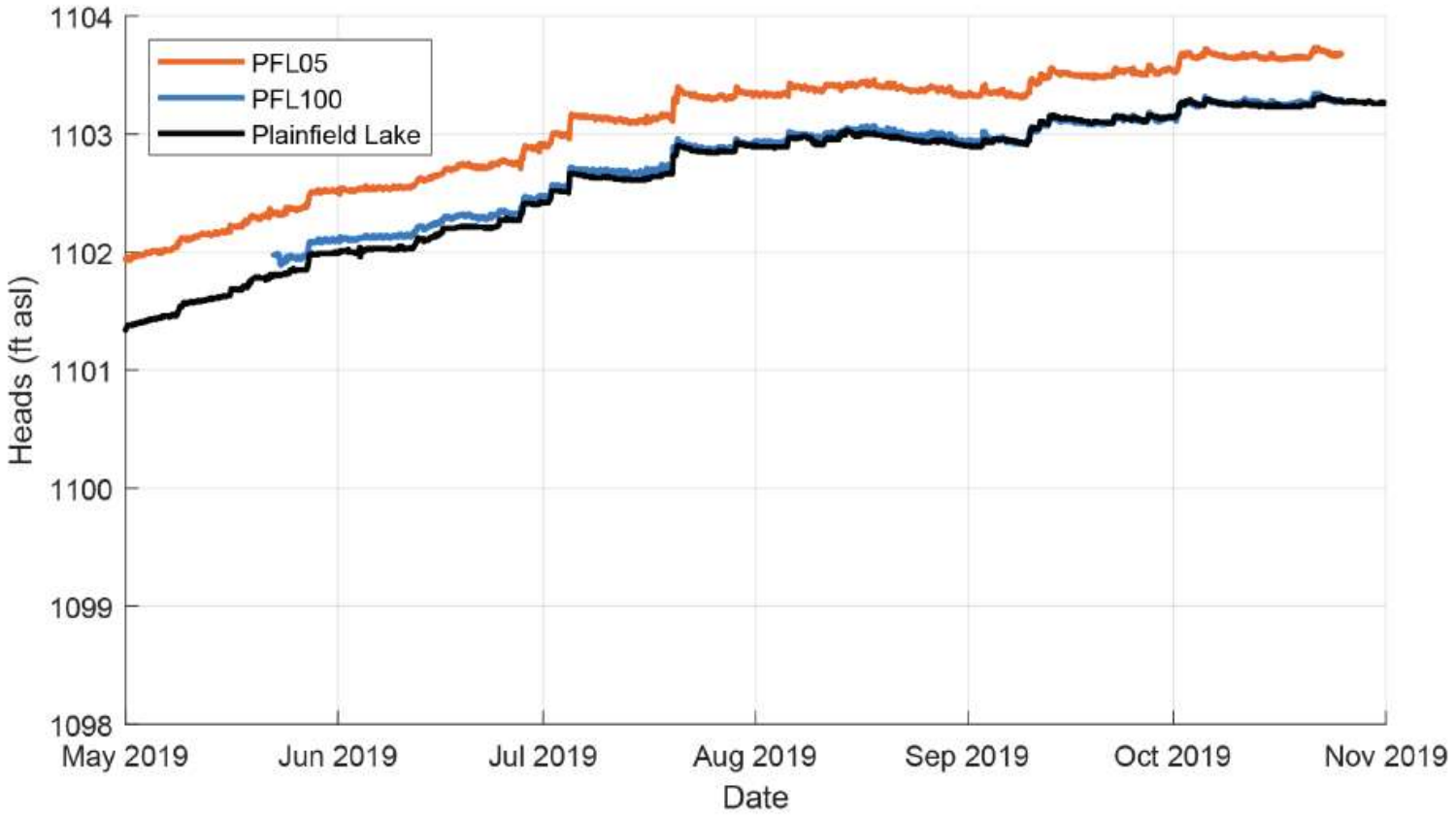

Figure 45. Hydraulic heads in monitoring well PFL05 and piezometer PFL100 as measured from spring to fall 2019. Lake-level elevation is shown in black, water table monitoring well is shown in orange, and deep piezometer is shown in blue.

湖泊床面水文

Figure 47. Lakebed piezometer and seepage meter inst

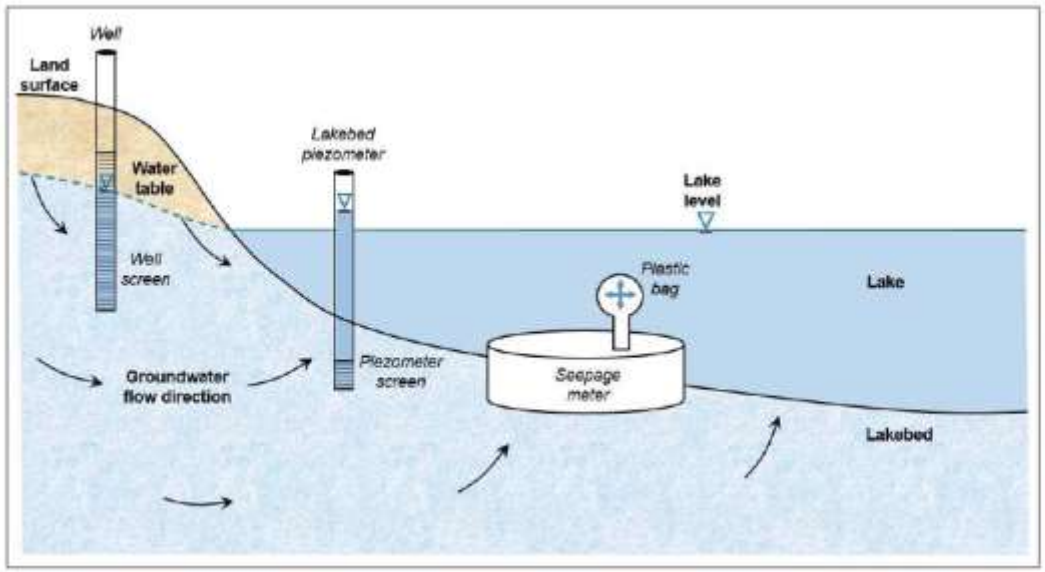

Figure 48. Illustration of a monitoring well, lakebed piezometer, and seepage meter deployed at a lake. Groundwater is shown

湖底的水力传导度

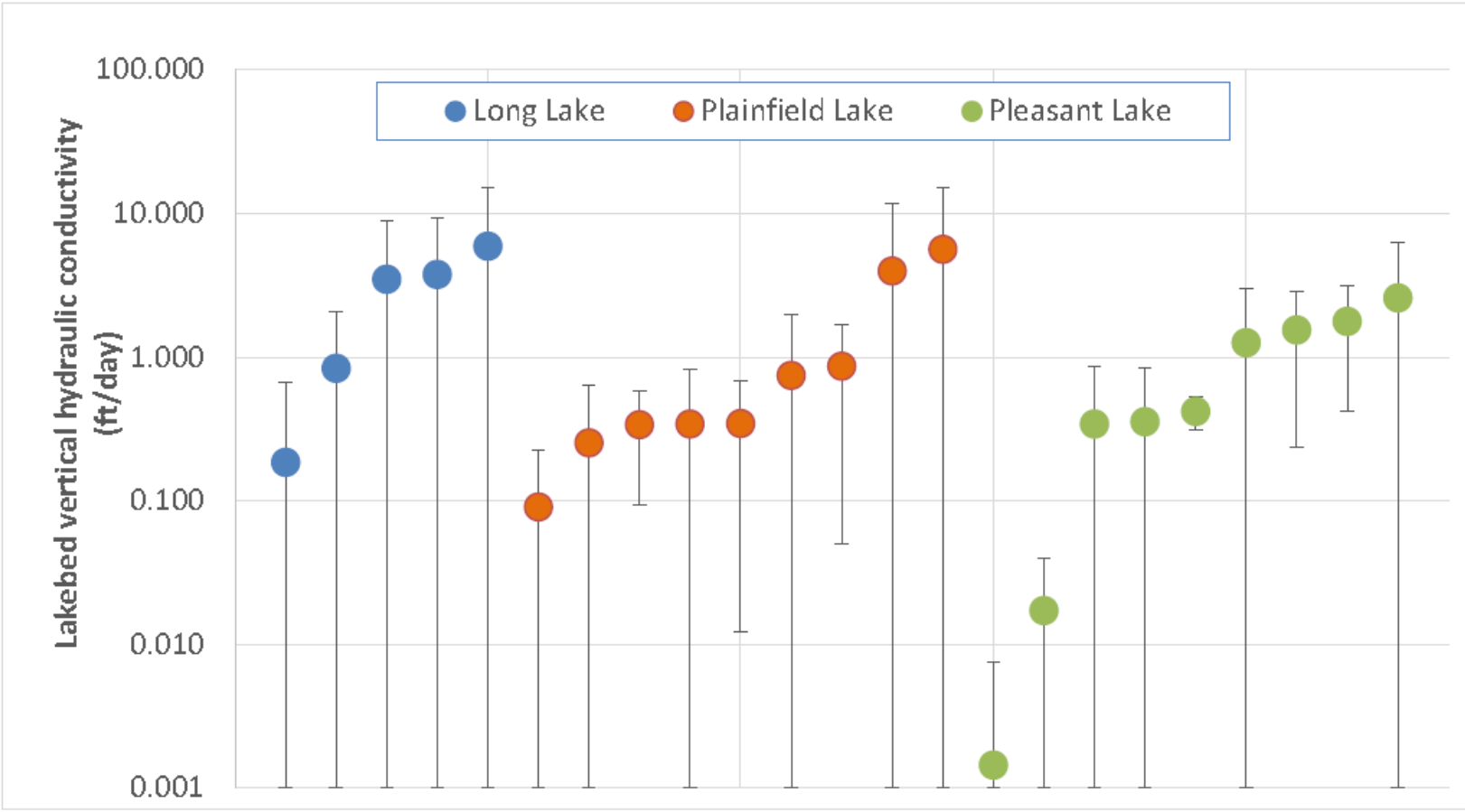

Figure 51. Lakebed vertical conductivity estimates determined from mini-piezometer and seepage meter data. Each lake is plotted in a different color; each dot represents the lakebed conductivity estimate at a location around the lakes. Error bars represent the combined error of seepage meter and piezometer measurements. Error bars terminate at K=0 as calculated hydraulic conductivities less than zero were not allowed.

水文地质—概念及创建分层

Central Sands研究区域的水文地质单元包括非固结的冰川泥沙和基岩单元。基岩分为：

1. Paleozoic sandstones
2. Paleozoic dolomites
3. Precambrian crystalline bedrock

图54显示Paleozoic砂岩和dolomite

图55显示基岩高程表面

图56显示了Precambrian基岩高程表面

ArcGIS处理数据创建基岩表面

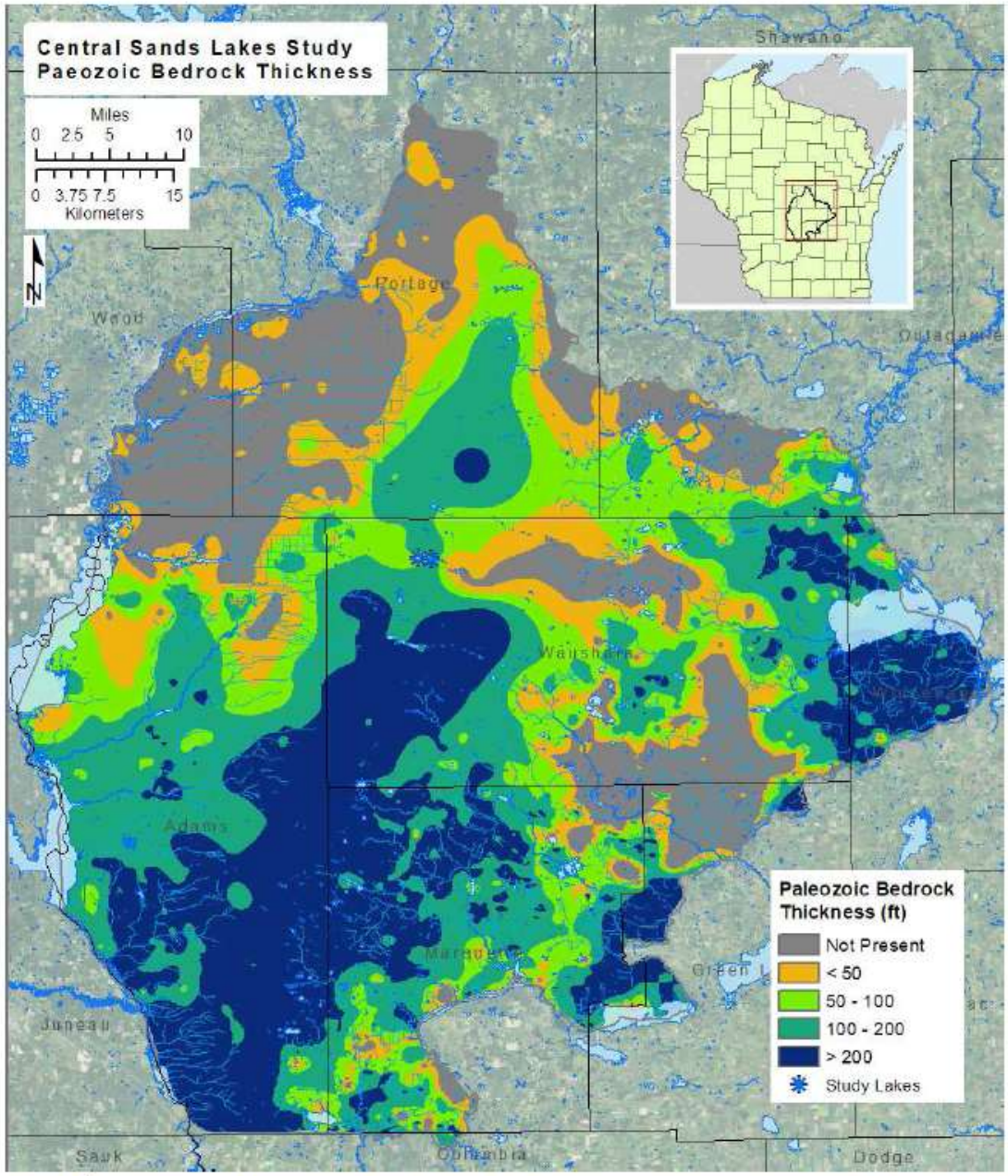

Figure 54. Thickness of Paleozoic bedrock, typically Cambrian sandstone except in the far eastern part of the CSLS model domain, where dolomite is present.

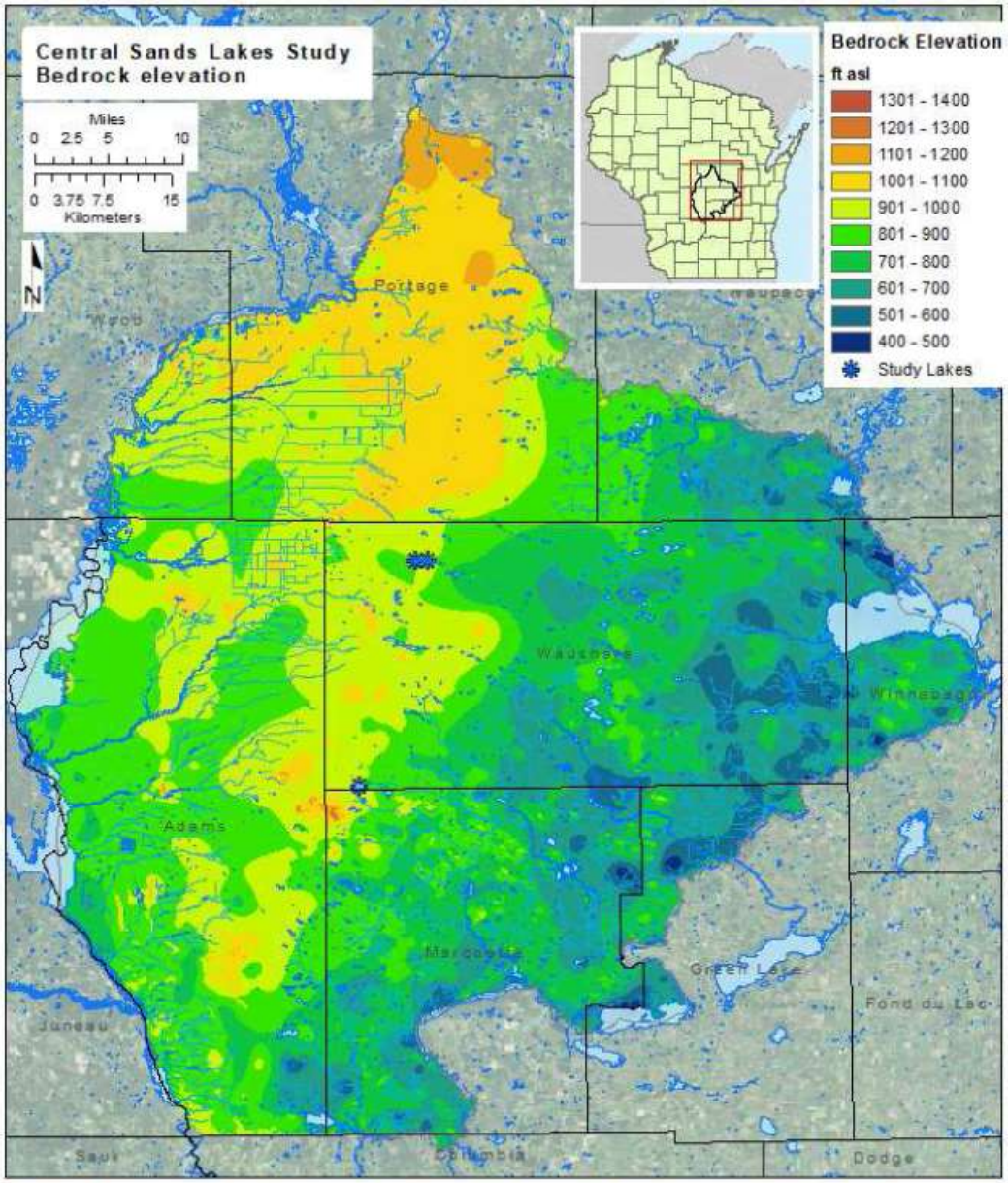

Figure 55. Bedrock surface elevation. Upper bedrock units include crystalline bedrock to the north, dolomite to the east, and sandstone over the majority of the model domain. Bedrock data points near the study lakes are shown in Figure 11.

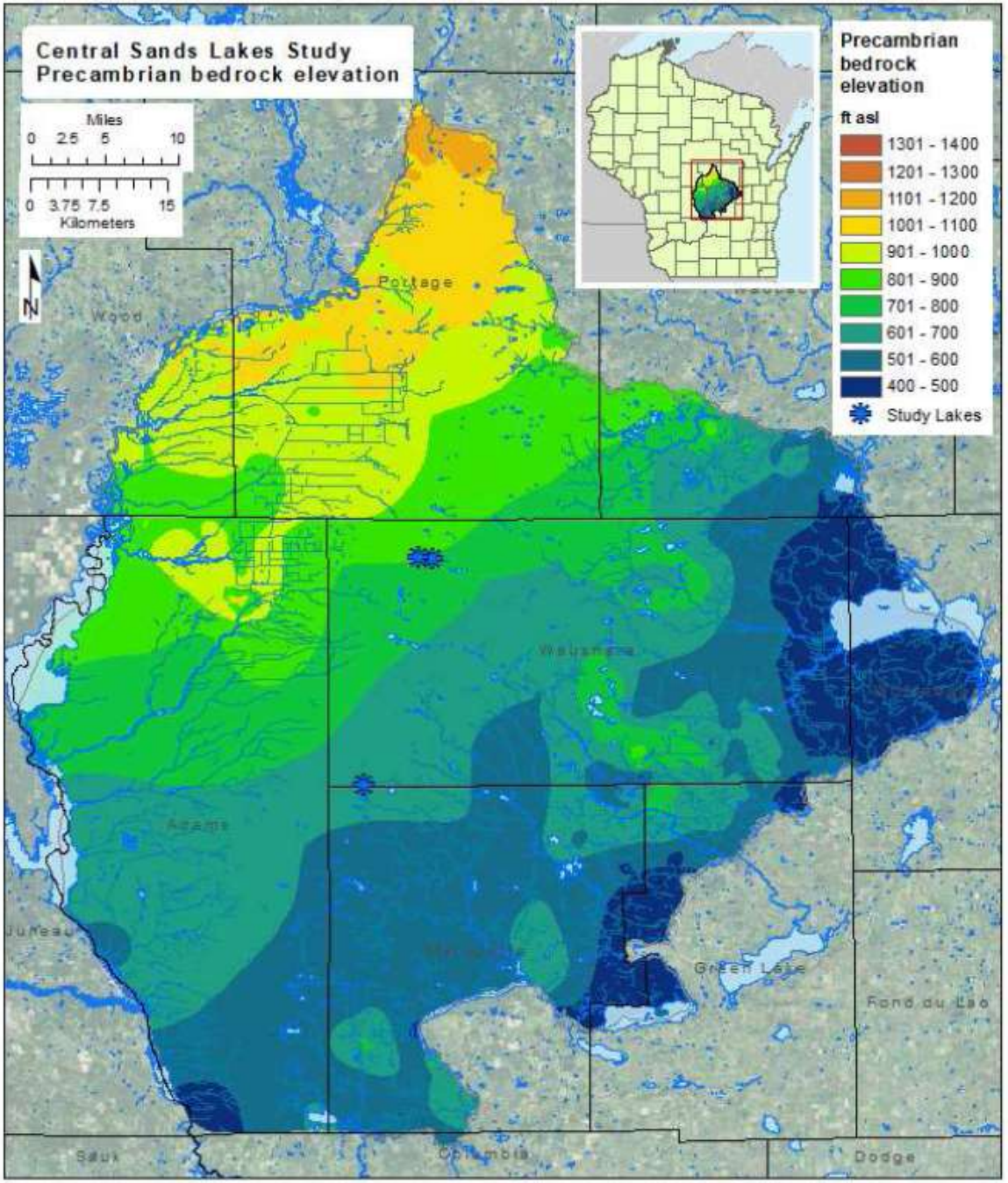

Figure 56. Precambrian bedrock surface elevation

数据高程和基岩深度分布。

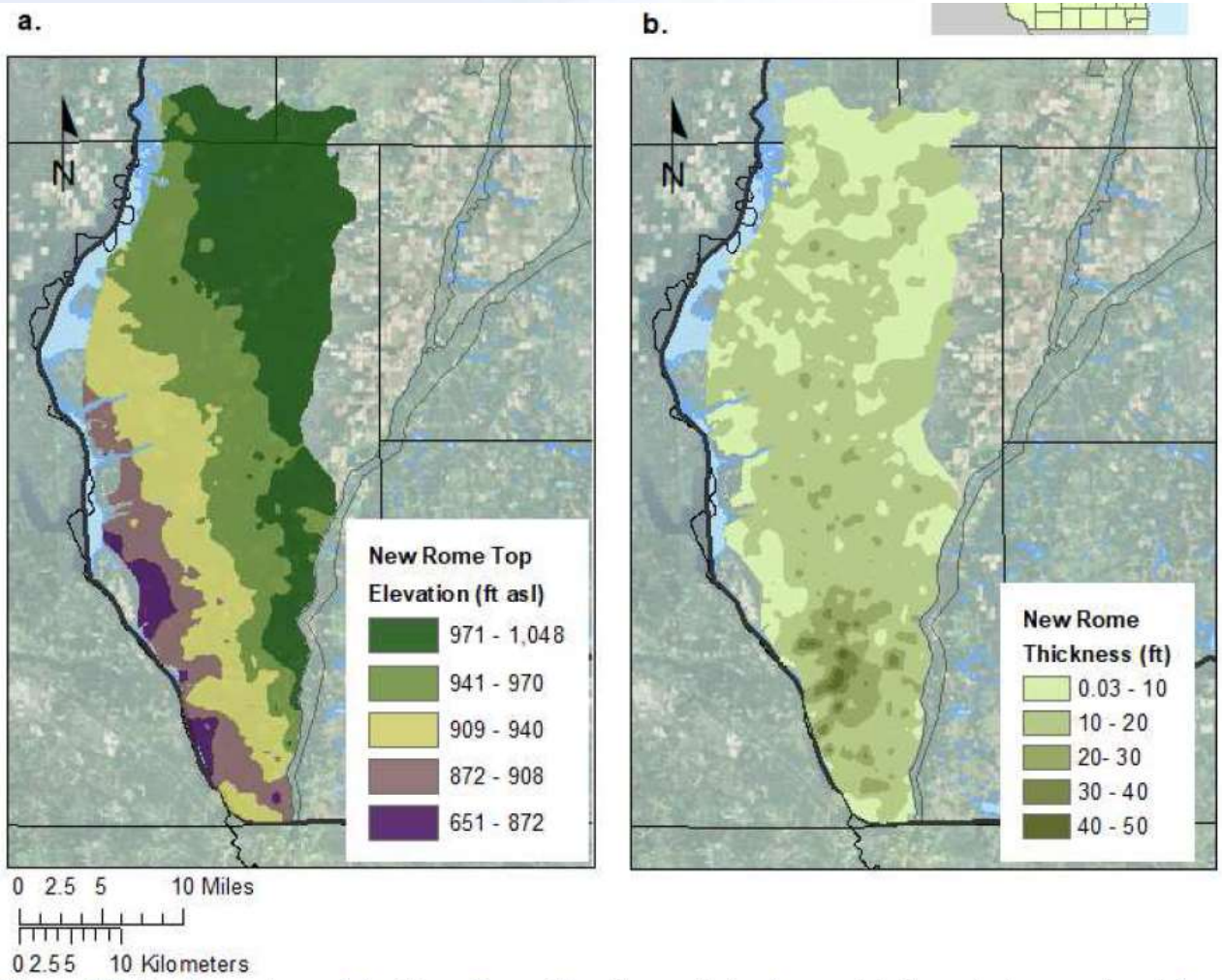

Figure 57. Configuration of the New Rome Member within the model domain interpolated from well construction and geologic log data. (a) Upper surface of the New Rome. The unit slopes to the southwest. (b) Thickness of the New Rome increases to the south. The unit becomes thin and discontinuous to the north and may be intermittently present north of the extent mapped.

创建分层—各向异性（水力传导度，空间插值）

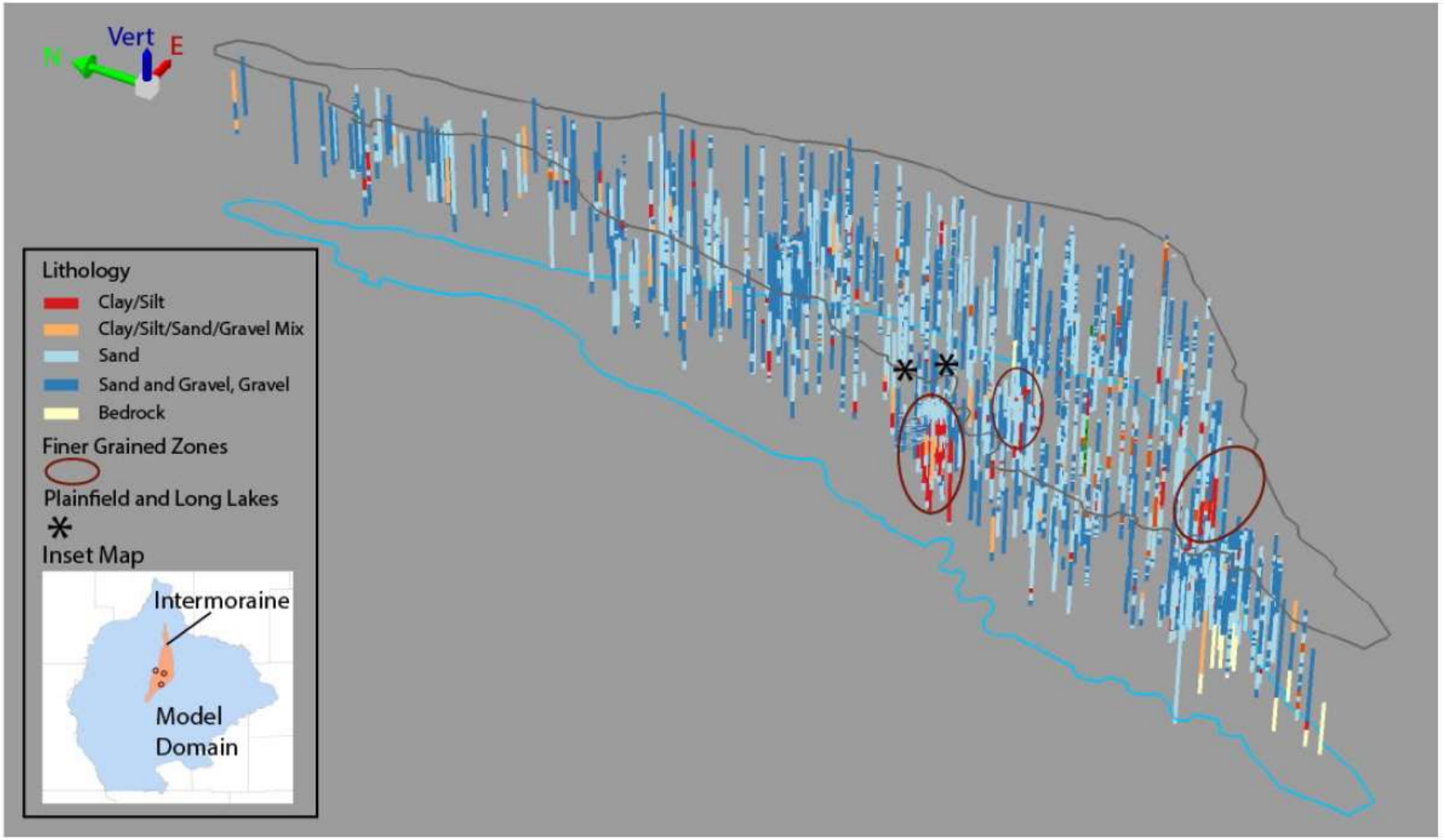

Figure 58. Northwest looking view of the well log lithologies in the intermorainal area. Area shown corresponds to the Intermoraine area in the inset map. In contrast to the outwash plain to the west, fine-grained sediments are fairly common at

横剖面水文地质

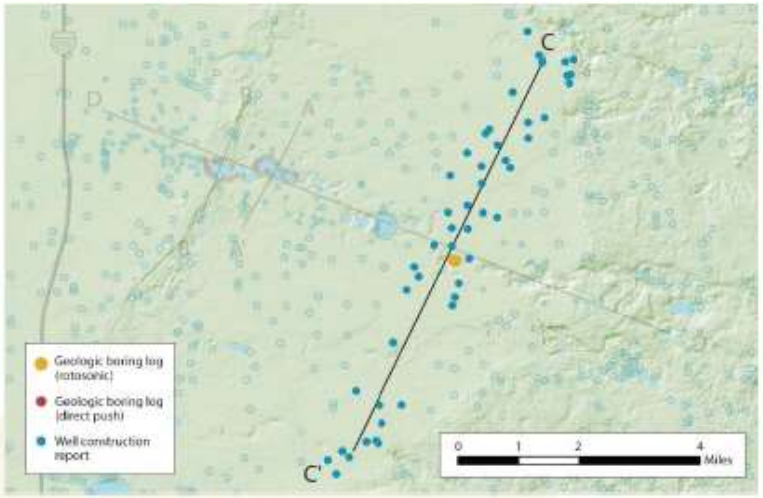

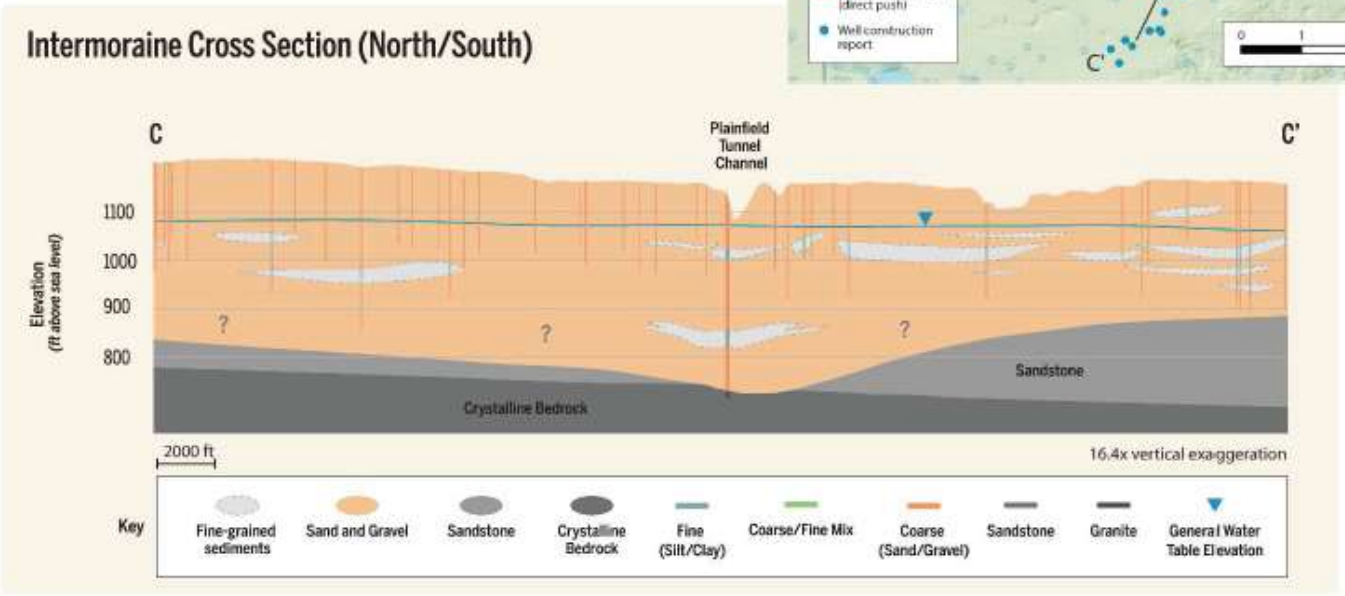

Figure 62. Conceptual cross-section perpendicular to the Plainfield Tunnel Channel at the eastern rotosonic site.

Hydrostratigraphy – Aquifer Properties

使用好几种方法计算了研究区域的含水层特性（水力传导度）。

Table 4. Summary of data types use for aquifer characterization, the appropriate use of the data (Data Quality), aquifer parameters derived from each data type, and the number of data points in each category (*n*).

Data Source	Method/Test	Data Quality	Aquifer Parameters	*n*
Historic Aquifer Tests	Slug Tests, Multi-well Pumping Tests	site specific	hydraulic conductivity, aquifer storage, anisotropy	70
Well Construction Reports/TGUESS	Specific Capacity Tests	regional estimation	Transmissivity → hydraulic conductivity, regional groundwater flow	36,220
CSLS monitoring well aquifer tests	Pumping Tests, Injection Tests	site specific, study area	hydraulic conductivity, groundwater flow and gradients	36
Investigative Borings - geophysical	Direct-Push Permeameter	site specific	bulk hydraulic conductivity, vertical conductivity distribution	4
Rotosonic core (east)	Grain-size Analysis	qualitative estimates	vertical conductivity distribution	1
Geologic logs, well construction logs	Sediment type classification: Coarse-fine analysis	qualitative regional estimation	spatial distribution of high- and low-conductivity sediment types, potential anisotropy distribution	12,938

总结

将观测和分析数据考虑到地下水模型中有助于深入理解地下水运行。

水文地质调查的主要目的就是：

获得基岩深度、含水层特性的3D空间分布；

水力传导度的确定。

泥沙特性？

地下水位观测（Darcy)

Pleasant Lake算例

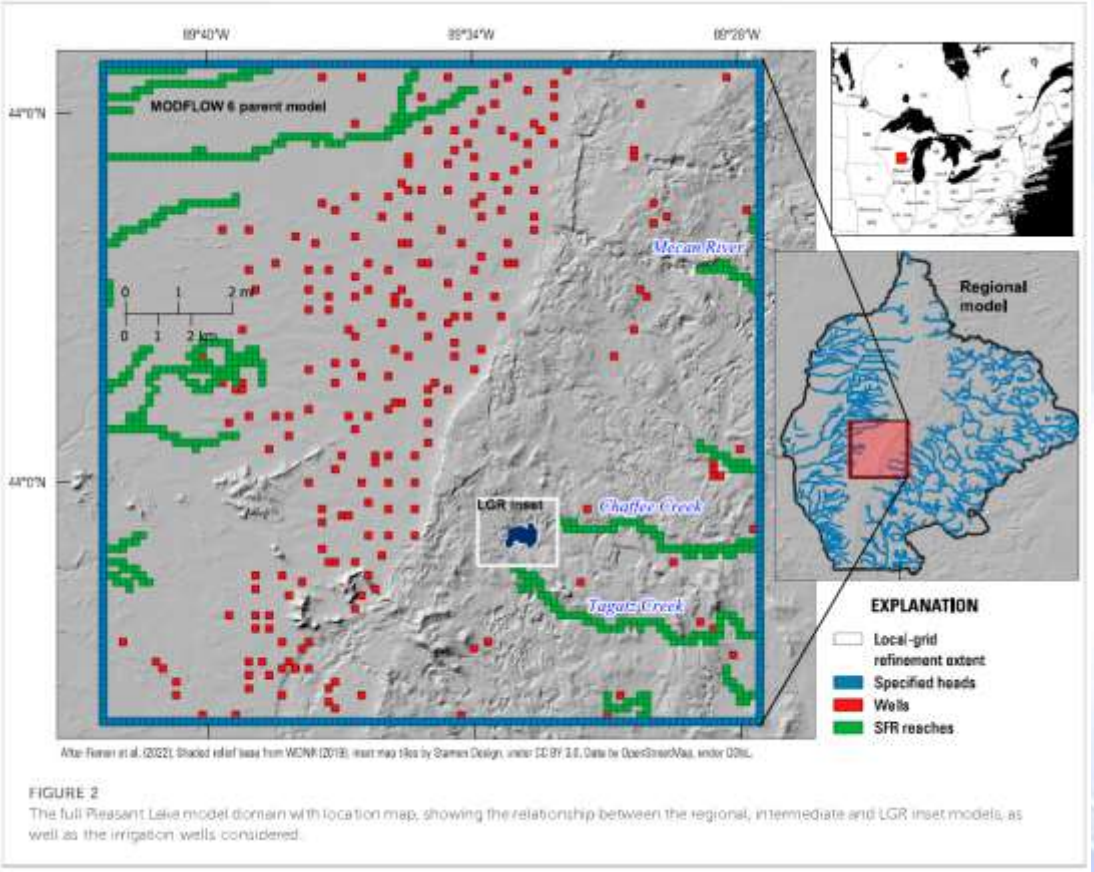

FIGURE 2
The full Pleasant Lake model domain with location map, showing the relationship between the regional, intermediate and LGR inset models, as well as the irrigation wells considered.

Pleasant Lake模型是Central Sands Lake 的一部分(Fienen et al., 2022)，研究地下水抽取和Wisconsin中央的一个湖泊生态功能之间的关系。

Pleasant Lake算例

需要多种尺度的模拟。Lake周围需要高分辨率对水位和地下水-湖泊通量的精确模拟。还需要大模型模拟远场水利用活动（主要是农业灌溉）。为此，联合3个模型：一个大范围的区域模型(MODFLOW-NWT)、一个区域模型内部的modflow6 inset模型、一个细化的modflow6模型（嵌套在中间模型内）。MODFLOW-NWT提供远场边界的地下水，与modflow6单向耦合，通过沿modflow6中间模型的周围边界的随时间变化的水头耦合。2个modflow6模型双向动态耦合地下水数值解，允许模型间的反馈。几个MODFLOW模型的地下水补给(recharge)的评估，由SWB模拟提供，表征各种气候和土地利用的假设情景。SWB模型提供净渗透评估，以NetCDF格式，直接被MODFLOW-setup读取，提供给MODFLOW模型的Recharge软件。

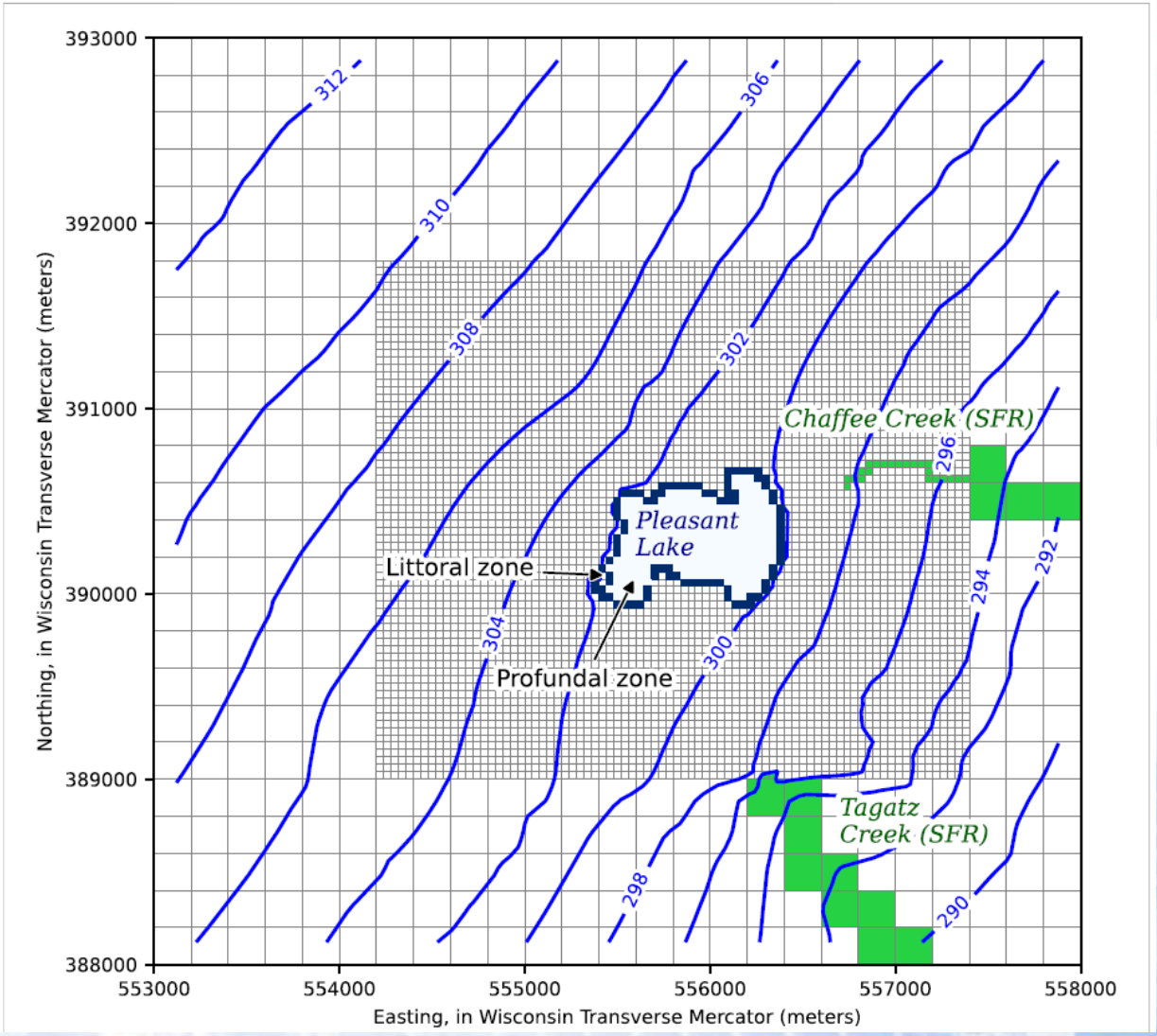

简单示例的Pleasant Lake模型如图3显示。